Agricultural and Forest Meteorology 204 (2015) 79–93

Contents lists available at ScienceDirect

Agricultural and Forest Meteorology

journal homepage: www.elsevier.com/locate/agrformet

Modeling spatial and temporal dynamics of wind flow and potential fire behavior following a mountain pine beetle outbreak in a lodgepole pine forest

Chad M. Hoffman[a,*], Rodman Linn[b], Russell Parsons[c], Carolyn Sieg[d], Judith Winterkamp[e]

[a] Department of Forest and Rangeland Stewardship, Colorado State University, 1472 Campus Delivery, Fort Collins, CO 80523, USA
[b] Earth and Environmental Sciences Division, Los Alamos National Laboratory, Los Alamos, NM 87544, USA
[c] USDA Forest Service Rocky Mountain Research Station Fire Sciences Laboratory, 5775 W US Highway 10, Missoula, MT 59802, USA
[d] USDA Forest Service Rocky Mountain Research Station, 2500 Pine Knoll Drive,Flagstaff, AZ 86001, USA
[e] Earth and Environmental Sciences Division, Los Alamos National Laboratory, Los Alamos, NM 87544, USA

ARTICLE INFO

Article history:
Received 4 August 2014
Received in revised form
30 December 2014
Accepted 30 January 2015

Keywords:
Turbulence
HIGRAD/FIRETEC
Fire behavior
Bark beetle
Heterogeneous fuels

ABSTRACT

Patches of live, dead, and dying trees resulting from bark beetle-caused mortality alter spatial and temporal variability in the canopy and surface fuel complex through changes in the foliar moisture content of attacked trees and through the redistribution of canopy fuels. The resulting heterogeneous fuels complexes alter within-canopy wind flow, wind fluctuations, and rate of fire spread. However, there is currently little information about the potential influence of different rates and patterns of mortality on wind flow and fire behavior following bark beetle outbreaks. In this study, we contrasted within-canopy wind flow and fire rate-of-spread (ROS) at two different ambient wind speeds using FIRETEC for two differing bark beetle attack trajectories for a lodgepole pine (*Pinus contorta*) forest. These two attack trajectories represent different realizations of a bark beetle outbreak and result in different amounts and patterns of mortality through time. Our simulations suggested that the mean within-canopy wind velocities increased through time following the progression of mortality. In addition, we found that for a given level of mortality, a bark beetle outbreak that resulted in a higher degree of aggregation of canopy fuels had greater mean within-canopy wind velocities due to the channeling of wind flow. These findings suggest that bark beetle mortality can influence the mean within-canopy wind flow in two ways: first, by reducing the amount of vegetation present in the canopy acting as a source of drag; and second, by altering spatial patterns of vegetation that can lead to channeling of wind flow. Changes in the fire rate-of-spread were positively related to the level and continuity of bark beetle mortality. Peak rates of spread were between 1.2 and 2.7 times greater than the pre-outbreak scenario and coincided with a high level of mortality and minimal loss of canopy fuels. Following the loss of canopy fuels the rate of fire spread declined to levels below the initial phases of the outbreak in low wind speed cases but remained above pre-outbreak levels in high wind speed cases. These findings suggest that the rate and pattern of mortality arising from a bark beetle outbreak exerts significant influence on the magnitude and timing of alterations to the within-canopy wind flow and rate of fire spread. Our findings help clarify existing knowledge gaps related to the effect of bark beetle outbreaks on fire behavior and could explain potential differences in the reported effects of bark beetle outbreaks on fire behavior through time.

1. Introduction

Native bark beetles (Coleoptera: Curculionidae, Scolytinae) are important disturbance agents of forests throughout North America. The mortality of trees during a bark beetle outbreak results in spatial alterations to forest structure, the fuels complex, and a variety of ecological processes across a wide range of temporal and spatial

* Corresponding author. Tel.: +1 970 491 1338.
E-mail addresses: c.hoffman@colostate.edu (C.M. Hoffman), rrl@lanl.gov (R. Linn), rparsons@fs.fed.us (R. Parsons), csieg@fs.fed.us (C. Sieg), judyw@lanl.gov (J. Winterkamp).

http://dx.doi.org/10.1016/j.agrformet.2015.01.018
0168-1923/

scales (Raffa et al., 2008). The collective influence of individual tree mortality affects the number as well as the size and age class distribution of living trees (Raffa et al., 2008). Changes in the structure of forest canopies through time result in altered gradients of foliar moisture contents and vertical and horizontal spatial arrangement of biomass that in turn influence the micro-climatic conditions within the stand. Altered stand structure, composition, and microclimate following bark beetle outbreaks can persist for tens of decades, thus, creating distinctive fuel and environmental conditions for wildfires through time. The recent extent of large-scale bark beetle-caused tree mortality across western North America has resulted in increased concern about the potential effect of bark beetle outbreaks on altered fuels complexes, the associated fire environment especially wind speeds and the potential fire behavior (Jenkins et al., 2008, 2012).

Although it has long been recognized that bark beetle-caused tree mortality may influence the fuels complex and subsequent fire behavior (Brown, 1975), only recently has the research community focused on quantifying such effects (Page and Jenkins, 2007; DeRose and Long, 2009; Klutsch et al., 2011; Simard et al., 2011; Hoffman et al., 2012a,b, 2013; Schoennagel et al., 2012; Donato et al., 2013; Linn et al., 2013). Individual attacked trees pass through an observable sequence of temporal phases, beginning with the green phase (healthy, un-attacked, and living trees), and progressing through red (dead, retaining foliage, and fine twigs), and gray phases (dead, with foliage and twigs having fallen to the ground). Other researchers (Jolly et al., 2012; Simard et al., 2011) have further separated the initial phases immediately after the initiation of the outbreak based on changes in foliar moisture content and the amount of canopy foliage that remains in the tree (e.g., very recently attacked trees that are beginning to lose canopy foliar moisture are often called yellow trees). Although the use of these temporal phases clearly shows how the fuels complex is altered at fine spatial scales associated with individual trees, alterations of the fuels complex at larger stand and landscape scales necessitates the spatial integration of such fine-scale changes across the stand. Complicating the ability to spatially integrate the effect of bark beetles on individual trees to larger areas is the fact that bark beetles have been shown to be selective in their attack strategy across stands and landscapes resulting in a mosaic of tree mortality (Bone et al., 2013), and that the mortality of individual trees within an area can occur over many years resulting in various mixtures of trees in different phases (Hicke et al., 2012). Stand and landscape-scale changes in the fuels complex, fire weather, and the potential fire behavior will therefore evolve following the initiation of an outbreak as a function of the rate and pattern of individual tree mortality. Yet very little work has attempted to quantify the effects of different rates and patterns of mortality on changes in the fuels complex, wind flow or fire behavior.

Previous simulation studies have suggested that changes in the fuels complex at the stand and landscape scales result in increased crown fire behavior for time periods immediately following the initiation of the outbreak when killed trees are in the red phase and there is a decrease in the mean foliar moisture content of the canopy (Page and Jenkins, 2007; Jenkins et al., 2008; Hicke et al., 2012; Hoffman et al., 2012a, 2013; Linn et al., 2013). Following the red stage, there is a decrease in crown fire potential when successfully killed trees have lost their foliage, and thus, reduced the stand level canopy fuel loading and increased the stand level canopy foliar moisture content (Page and Jenkins, 2007; Jenkins et al., 2008; Klutsch et al., 2011; Hicke et al., 2012; Simard et al., 2011; Schoennagel et al., 2012). However, substantial gaps in our knowledge remain with respect to the role that temporal and spatial variation in mortality may have on the fuels complex, fire environment, and potential fire behavior. This knowledge gap is due, in part both, to a lack of empirical or experimental data in bark beetle-affected forests and to limitations of models being used to explore these influences. Much of the past research directed at this knowledge gap has been done with modeling systems based on linkages between Rothermel's (1972, 1991) surface and crown fire spread models and Van Wagner's (1977) crown fire initiation and spread models. Modeling systems based on these linkages do not account for the spatial heterogeneity of the fuels complex, the influence of the fuels complex on the spatial and temporal variability in wind flow, or the effect of fire-induced turbulence; thus, these models are limited in their ability to offer further insights into the potential role of spatial heterogeneity arising from various rates and magnitudes of bark beetle mortality on fire behavior.

Process or physics-based fire behavior models such as the Wildland–Urban-Interface Fire Dynamics Simulator (WFDS, Mell et al., 2007, 2009) and HIGRAD/FIRETEC (Linn, 1997; Linn and Cunningham (2005); Linn et al., 2005; Pimont et al., 2009), hereafter referred to as FIRETEC, have been recently developed with the purpose of modeling many of the physical phenomena and interactions that control the behavior of a wildfire. Models such as WFDS and FIRETEC explicitly resolve a coupled set of partial differential equations describing the major physical processes and their interactions that influence fire behavior as well as the vertical and horizontal heterogeneity of the fuels complex within a three dimensional grid. Such modeling frameworks allow for the constantly changing, interactive relationship between the fire, the environment, and fuels to be simulated and can provide a framework to begin to explore the effect of various spatiotemporal fuels complexes following bark beetle mortality on potential fire behavior. A detailed description of the theoretical and mathematical concepts in FIRETEC can be found in Linn (1997), Linn et al. (2005), Linn and Cunningham (2005), and Pimont et al. (2009); more detailed information on WFDS can be found in Mell et al. (2007, 2009). To date, only a few studies have used physics-based models to investigate the potential effects of heterogeneity in the fuels complex arising from bark beetle mortality on fire behavior. Hoffman et al. (2012a, 2013) used WFDS to investigate the effect of the magnitude of bark beetle mortality, the spatial arrangement of overstory trees, and the surface fireline intensity on fire behavior during time periods when there are mixtures of individual trees in the red and green phases. Their results suggested that the crown fire intensity and amount of canopy fuel consumption increased as a function of the level of mortality and that this effect was most pronounced under moderate conditions. Linn et al. (2013) utilized FIRETEC to investigate changes in wind flow and fire rate-of-spread along a temporal sequence following bark beetle mortality in highly heterogeneous pinyon–juniper *(Pinus edulis–Juniperus* spp.) woodland. Their results suggested that alterations in the heterogeneity of canopy foliar moisture resulted in increased fire rates-of-spread during the initial phases of an outbreak and the heterogeneous fuels complex resulting from bark beetle mortality altered wind flow and fire behavior for periods of time when there was a mixture of green and gray trees. Past studies such as these highlight the potential role of physics-based models to investigate the implications of heterogeneity on fire behavior following disturbances such as bark beetle outbreaks.

In this paper, we used field data to populate a simple probabilistic model for tree-to-tree beetle spread and attack to develop two attack trajectories. These two attack trajectories represented two spatial and temporal patterns of bark beetle mortality with different mixtures of individual trees in various phases. The first scenario represented a rapid, broad-scale mortality event that resulted in high rates of mortality over a short period of time and a stand structure that is best characterized as random or dispersed through space. In contrast, the second scenario had a lower overall rate of mortality over a longer temporal period that resulted in clumpy patches of aggregated tree mortality, and thus, more

heterogeneous forest structure at the landscape scale. We then developed an analogous forest in FIRETEC, a physics-based model that has been fully coupled to an atmospheric hydrodynamics model, HIGRAD. Using this coupled model we examined how different levels, rates and patterns of bark beetle mortality influenced fire/vegetation/atmosphere interactions and potential fire behavior in lodgepole pine (*Pinus contorta*)-dominated forests.

2. Methods

To investigate the potential effects that the rate and spatial pattern of mortality has on post-outbreak wind fields and fire behavior, we used field data collected by Reinhardt et al. (2006) to develop an analogous pre-outbreak forest that spanned across a 400-m × 400-m × 480-m domain. The analogous pre-outbreak forest was developed based on individual tree level data collected in 2000 and 2001 on a 10-m radius, circular plot (0.03 ha) located in the Tenderfoot Creek Experimental Forest on the Lewis and Clark National Forest in Montana (Scott and Reinhardt, 2001; Reinhardt et al., 2006). In addition to standard individual tree data (height, diameter at breast height, crown width, and canopy base height), canopy fuel biomass for several fuel categories were quantified via destructive branch sampling and direct measurement. Regression equations were developed from sub-samples to predict biomass quantities for each individual tree in the stand (Keane et al., 2005; Reinhardt et al., 2006). Using the individual tree data collected by Reinhardt et al. (2006) we generated an analogous forest with the same properties as those measured by replicating the individual tree data and randomly assigning *x* and *y* coordinates for each tree from a Poisson probability distribution within the minimum and maximum domain boundaries to achieve similar tree densities as measured in the field. The simulated analogous pre-outbreak forest consisted of 2132 trees per hectare with a stand level basal area of 42.7 m^2 ha^{-1}, a positively skewed diameter distribution with a quadratic mean diameter of 15.5 cm, a mean tree height of 10.9 m, and a mean crown base height of 6.6 m.

Using this analogous forest we then simulated two different bark beetle outbreaks using a probabilistic spatially explicit bark beetle-mortality model. The first outbreak scenario represented a stand-scale eruption of bark beetles resulting in rapid and broad-scale mortality, and the second mortality scenario resulted in a less rapid rate of mortality with the formation of pockets of mortality that grew through time and eventually merged together. These two scenarios are referred to as the Rapid/Broad and Slow/Patchy scenarios, respectively.

In reality, successful propagation of beetle attacks through a forest is extremely complex, with numerous biotic and abiotic factors, which are themselves dynamic in space and time, interacting to influence the propagation of beetles across a landscape. Models characterizing different beetle attack mechanisms have been developed with varying degrees of detail (e.g., Geiszler et al., 1980; Safranyik et al., 1989); more detailed models often require inputs such as individual tree vigor, beetle population demographics, and concentrations of pheromone clouds (Logan et al., 1998). As these quantities can be difficult to measure, practicality often necessitates simpler models that are more easily applied with readily available data. As our primary interest in this study was in the effects of tree mortality resulting from a bark beetle outbreak on the fuels complex, wind flow, and fire behavior, rather than the attacks themselves, we developed a simple model that can easily be applied to a forest stand using two factors: (1) because successful attacks depend on pheromone plume concentrations, which decrease with distance from the host tree, the likelihood of beetle attack on any new tree increases with proximity to the host tree (Johnson and Coster, 1978; Geiszler and Gara, 1978; Mitchell and Preisler, 1991); and (2) beetles preferentially attack larger diameter trees as the thicker phloem provides greater nutritional content (Negrón and Popp, 2004; Graf et al., 2012). Both factors are modeled as probability functions; one defining the probability of a given tree being successfully attacked based on the diameter at breast height (*P*-diam) and the second defining the probability of attack based on the distance from a beetle host tree (*P*-dist). Both probability distribution functions are variants of a logistic form with P_{diam} and P_{dist} of the forms shown in Eq. (1) and (2).

$$P_{\text{diam}} = a(1 + b \times e^{(-c \times D)}) \quad (1)$$

$$P_{\text{dist}} = \frac{1 - (1 - f)}{1 + g \times e^{(-h \times R)}} \quad (2)$$

where *D* is the diameter at breast height (cm) of a tree and *R* is the distance from the tree of interest to a specific tree that has been infected one year earlier.

In Eq. (1) and (2), the parameters *a* and *f* set asymptotic limits for the probability functions as tree diameter, and distance from the host tree increases. Parameters *b*, *g*, *c*, and *h* set the scaling and curvature of the exponential dependence on diameter and distance. Studies examining past outbreaks demonstrate that attack trajectories, in terms of mortality rates and impacts to tree populations, can vary significantly between sites, and in response to different biotic (e.g., beetle population dynamics) or abiotic (e.g., climate and biophysical setting) factors (Cole and Amman, 1980; Logan et al., 1998). We did not have access to a complete beetle attack spatial time series dataset for robust model parameterization, so instead we chose values that result in two different trajectories that are qualitatively similar to observed beetle attacks over time (Cole and Amman, 1980) and which have parameters reasonably consistent with previous studies (Geiszler and Gara, 1978, Cole and Amman, 1980) (Table 1).

The final probability for successful attack, $P_{\text{mortality}}$, is defined as the product of P_{diam} and P_{dist} (Eq. (3)).

$$P_{\text{mortaliy}} = P_{\text{diam}} \times P_{\text{dist}} \quad (3)$$

Consistent with typical dynamics for the mountain pine beetle, a single generation of attacks occurs each year, and only recently killed trees (within one year) may serve as host trees for subsequent beetle attacks. Thus, the probability of one tree being attacked from a particular host is calculated once representing the integral probability over this one year after the host tree was killed.

Potential fire behavior was simulated for the no-mortality scenario (year 0), years 1–6 for the Rapid/Broad scenario and years 2, 5, 7, 9, and 15 for the Slow/Patchy scenario using FIRETEC. The simulation domain was a 400-m × 400-m × 480-m, divided into a 3D array of cells that are 2 m on the horizontal sides and vertically stretched so that they are approximately 1.5 m in height near the ground. All simulations were performed with a Rayleigh damping

Table 1
Parameters used in two simple stochastic simulations of tree-to-tree beetle spread.

	Tree diameter parameters			Distance from host parameters			
Scenario	*a*	*b*	*c*	*f*	*g*	*h*	Initial hosts (%)
Rapid/Broad	0.95	15.5	0.5	0.0	6.5	0.95	10%
Slow/Patchy	0.95	14.4	0.3	0.0	6.5	0.95	0.3%

layer along the top boundary. For each year following the initiation of the outbreak we simulated two different aloft wind speeds, 12 m s^{-1} and 24 m s^{-1} at a height of 450 m above the ground with neutral atmospheric conditions (referred to as low and high wind speed cases, respectively). Thus, the dominate driver of local very-near-canopy turbulence is dominated by the heterogeneous nature of the canopy. The initial inflow and boundary conditions, including the mean velocity and turbulent fluctuations for each simulation, were pre-computed following Pimont et al. (2011) and Cassagne et al. (2011). This method develops turbulent wind fields for use as initial inflow and boundary conditions by simulating wind flow, without a fire, through the analogous forest with cyclic boundary conditions for all lateral, upstream and downstream boundaries. The dynamic wind sets developed for each mortality stage were then used as the inlet conditions for simulating potential fire behavior. As shown by Linn et al. (2013), variations in canopy structure created at various times following a bark beetle outbreak can generate different wind velocity and turbulence profiles within and just above the canopy, even though all scenarios within respective low and high wind cases have similar wind speeds far above the canopy. Although other factors such as reduced water mass, changes in albedo, and evaporation associated with tree mortality may impact local wind flow we did not consider these factors in our modeling approach.

The distribution of fine fuels within an individual tree crown was simulated using a series of parabolic profiles based on the tree's attributes following Linn et al. (2005). Because larger diameter woody crown fuel components (>2 mm) are considered to contribute little to the spread or intensity of crown fires (Rothermel 1983) our simulated crowns only consisted of fine fuels <2 mm such as needles and small twigs. The pre-outbreak surface fuels were simulated as a layer of fine fuels with a loading of 0.78 kg m^{-2} as measured by Reinhardt et al. (2006) and a surface area to volume ratio of 6470 m^2 m^{-3} (Brown, 1970), in a manner consistent with Linn et al. (2005). We simulated the fuels changes arising in a successfully beetle-killed tree with the following progression through time: (1) in the year that mortality occurs, trees were considered to be in the yellow phase and were simulated with all of the pre-outbreak canopy biomass and a foliar moisture content of 50%; (2) in the 2nd year after mortality trees were considered to be in the red phase and were simulated with all of their pre-outbreak canopy biomass and a foliar moisture content of 15%, comparable to recent empirical measurements (Jolly et al., 2012); (3) in the 3rd year following mortality trees were considered to be in the brown phase and were simulated with half of their pre-outbreak canopy biomass still in the canopy and a crown foliar moisture content of 15%; and (4) in the 4th year following mortality trees were considered to be in the gray phase and were simulated as having no canopy biomass. In a given year, all non beetle-killed trees were considered as alive and were simulated with their pre-outbreak canopy biomass and a foliar moisture content of 100%, consistent with live fuel moistures in drought conditions. As crown biomass was removed from beetle-killed trees it was transferred to the surface fuel layer underneath the crown. To isolate the potential effects of beetle-kill induced fuel changes, the only changes in the surface fuels following mortality were due to biomass lost from overstory trees as a result of their mortality. Thus, we did not account for changes in surface fuels due to litter fall from living trees, decomposition or vegetative responses to altered environmental conditions created by bark beetle mortality, such as colonization and growth by new trees. The moisture content of the surface fuels layer was assumed to be 5% in all simulations. To initiate a fire event in each scenario we simulated ignition by initiating, a 200-m long fire 100 m from the upwind boundary. These conditions were used to represent a free burning fire under drought conditions in a neutral atmosphere during the fire season.

For each simulation, the turbulence statistics for the non-fire induced winds were generated by spatially and temporally averaging over a 10-m wide strip across the width of the domain (200 cells wide) for 400 s near the inlet of the domain. This is similar to averaging over a single line 2 km long for 400 s. Normalizing the correlations between the velocity fluctuations by the mean velocity squared, provides a quantity that helps compare the kinetic energy associated with fluctuations in various directions and the mean kinetic energy, which is all in the streamwise direction since the mean crosswind and vertical wind speeds are zero. The propagation distance of the fire following ignition was determined by identifying the farthest downwind location where the resolved fuel

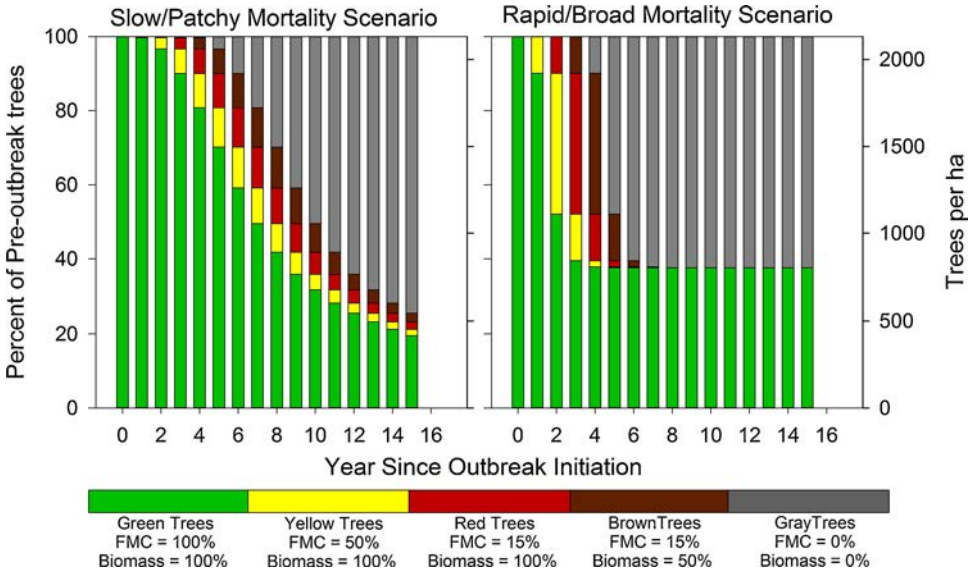

Fig. 1. Temporal progression of tree classes following the initiation of a bark beetle outbreak for the Slow/Patchy and Rapid/Broad mortality scenarios. Individual tree classes simulated represent a progression from live un-attacked trees (green trees), recently attacked (first year) trees with fading crowns (yellow trees), attacked trees with low foliar moisture contents and no loss of canopy foliage (red trees), attacked trees with low foliar moisture contents and the loss of 50% of the canopy foliage (brown trees), and attacked trees that have lost all of their canopy foliage (gray trees). (For interpretation of the references to color in this figure legend, the reader is referred to the web version of this article.)

temperature exceeded 500 K at a frequency of 1 Hz. The mean rate of spread (ROS) was estimated as the slope of a least squares fit to the propagation distance vs. time curve as the fire traveled from 50 to 250 m downwind of the ignition line.

3. Results and Discussion

3.1. Simulated changes in the fuels complex

The tree-to-tree beetle attack model that was used resulted in considerable temporal and spatial variations in the simulated stand structure and mortality-stage composition following the initiation of the outbreak. These variations reflected differences between the rates of overstory tree mortality simulated in the Slow/Patchy and Rapid/Broad scenarios (Fig. 1).

The Slow/Patchy mortality scenario represented a bark beetle outbreak that was more gradual and severe in nature, killing approximately 80% of all pre-outbreak stems over a 15-year period. The propagation of mortality in this scenario across the landscape appeared as a series of large fronts spreading radially from the infested trees, resulting in the formation of a matrix of clumps of un-attacked live trees and gaps of recently killed trees that have lost their needles. In contrast the Rapid/Broad mortality scenario represented a bark beetle outbreak that was much more abrupt and ultimately less severe with approximately 63% of all pre-outbreak stems being killed over a 6-year time period (Fig. 1). The difference in mortality level for the Rapid/Broad scenario was due to the probabilistic nature of the mortality model, where not all trees near a host became infested and small trees preferentially survived. The resulting forest structure showed that about one third of the lodgepole pines became surrounded by red, brown or gray trees or subalpine fir *(Abies lasiocarpa)* and were shielded from future infestations. In addition to the differences in overall mortality levels, the Rapid/Broad outbreak resulted in the loss of a greater proportion of large trees than the Slow/Patchy outbreak. The results of this trend were that the Rapid/Broad outbreak left a stand structure that included a greater number of small lodgepole pines; whereas the Slow/Patchy outbreak eventually resulted in a stand with much fewer but larger lodgepole pines surviving.

Given the different rates of mortality between the two scenarios it is not surprising that the temporal dynamics of the fuels complex were also different between the two scenarios. Both scenarios showed a trend of increasing surface fuel load and decreasing canopy fuel load through time as hypothesized by Jenkins et al. (2008) and Hicke et al. (2012). However, due to differences in the size of trees killed during between the two scenarios, the same level of mortality (measured in terms of number of trees killed) did not necessarily result in the same level of surface fuel loading, canopy fuel loading or mean canopy foliar moisture content (Fig. 2). For example, the mean canopy and surface fuel loading in the Rapid/Broad outbreak in year 6 and the Slow/Patchy outbreak in year were nearly equivalent, however, the Slow/Patchy outbreak scenario had almost 20% more mortality (Fig. 2). The Rapid/Broad scenario had a lower mean canopy foliar moisture content through the first five years compared to the Slow/Patchy scenario, due to the greater proportion of attacked trees with dead needles remaining.

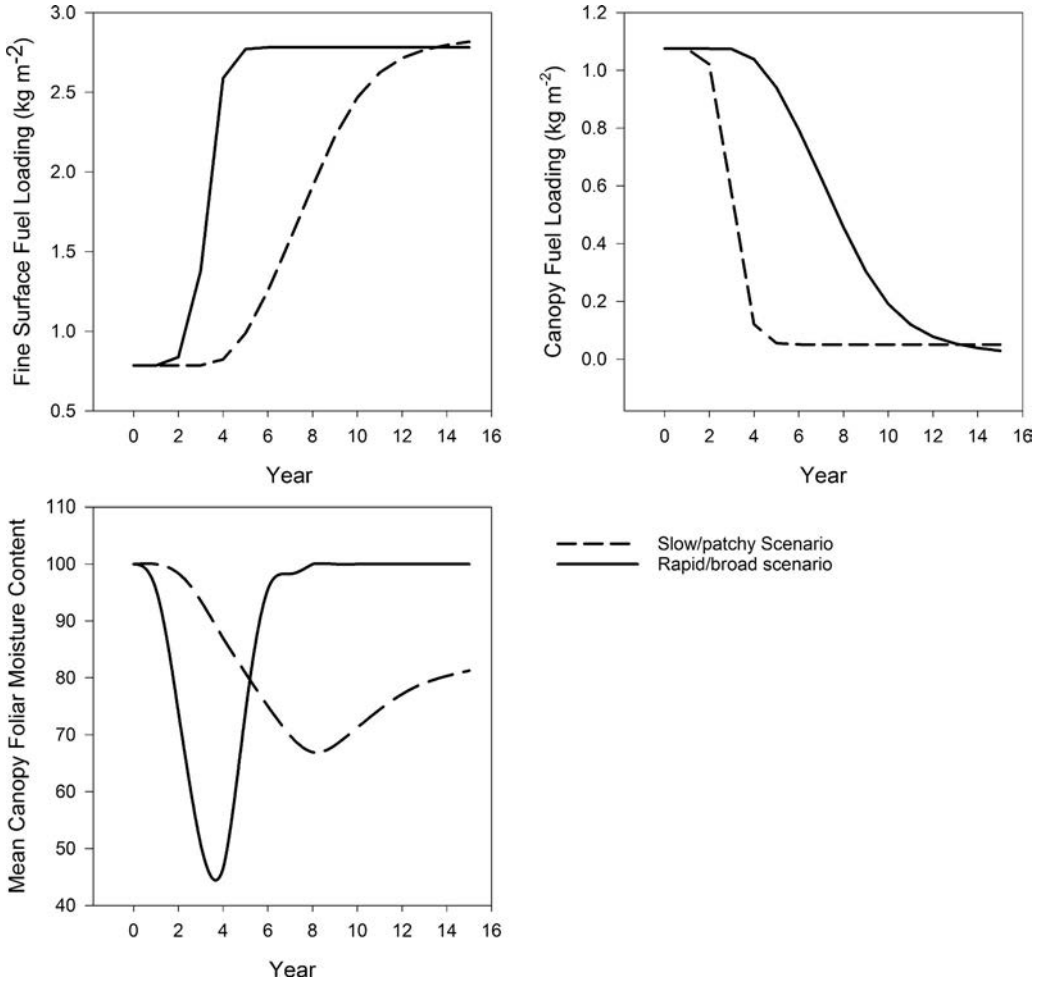

Fig. 2. Changes in surface fuel loading, canopy fuel loading and mean canopy foliar moisture content through time for the Rapid/Broad and Slow/Patchy scenarios.

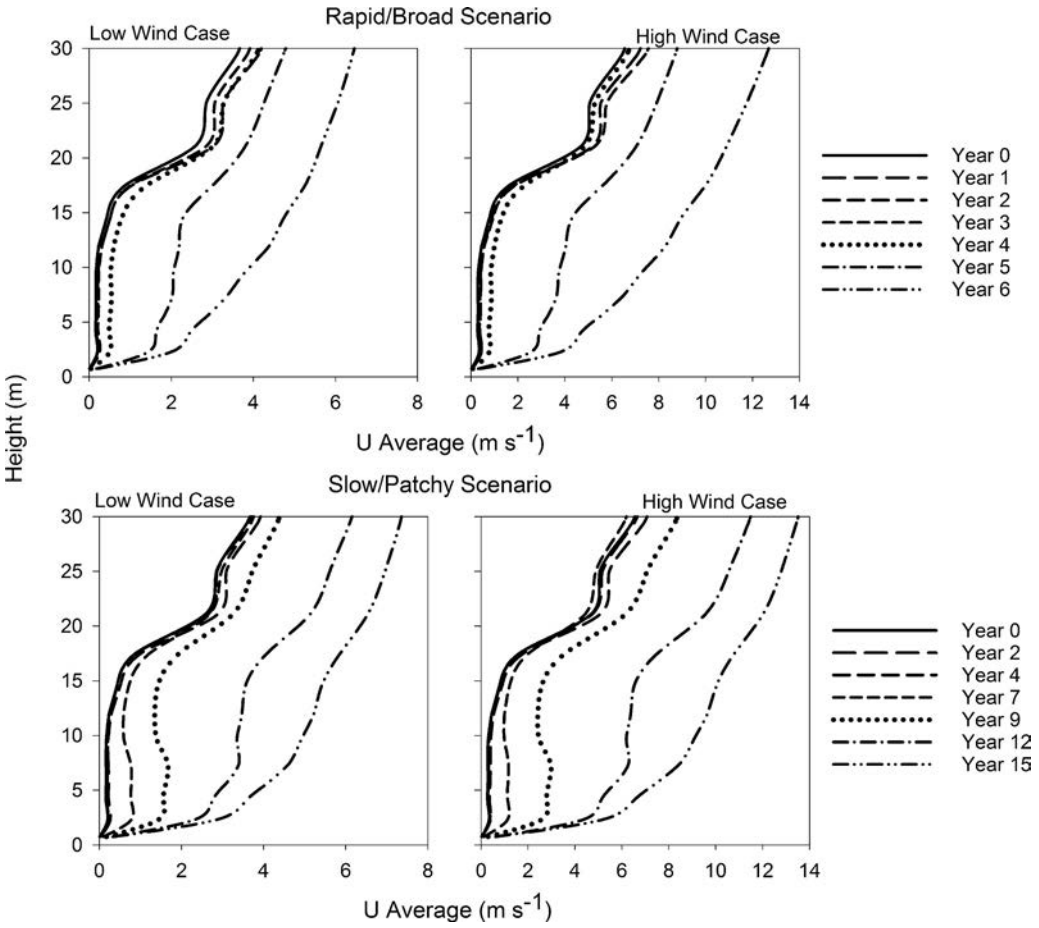

Fig. 3. Vertical profiles of the streamwise wind velocity for the Rapid/Broad and Slow/Patchy scenarios for both the low and high wind speed cases. Low wind speed scenarios are presented in the left column and have different scales along the x axis compared to the high wind speed scenarios (right hand column).

Following year 5 the Slow/Patchy outbreak had lower mean canopy foliar moisture content values due to the ongoing mortality and the continued presence of trees in the yellow, red and brown phases and the loss of dead foliage from the canopy in the Rapid/Broad scenario. These findings highlight the potential implications that the rate of mortality can have on the fuels complex through time and suggest that broad-scaled classification of bark beetle mortality based only on the time since the initiation of the outbreak or based on a combination of time since outbreak and the severity of the outbreak may not fully capture differences in fuel loading that can arise from various rates of mortality or differences in the size of attacked trees.

3.2. *Effect of beetle attack progressions on simulated changes in ambient winds*

The loss of needles over time due to mortality affected the magnitude of the mean wind speed as well as the shape of the wind velocity profile through the canopy (Fig. 3). The mean wind velocity increased as the bark-beetle outbreak progressed through time and canopy fuels were removed and deposited on the forest floor (Fig. 3). The Rapid/Broad scenario, which is characterized by a pulse of mortality followed by a sudden decrease in canopy fuels, had increased streamwise wind velocities within and below the canopy through the first six years of simulated mortality whereas the Slow/Patchy scenario had continued evolution of the within-canopy streamwise wind velocities through year 15. The shape and magnitude of the wind profiles showed minimal change until year 4 in the Rapid/Broad scenario and year 7 in the Slow/Patchy scenario with subsequent years showing a more dramatic increase in wind velocities and a wind profile shape that is best characterized as a logarithmic profile (Fig. 3).

The streamwise wind profiles normalized by the average streamwise wind at the top of the canopy suggested that as the mortality progressed, below-canopy wind speeds increased compared with the winds at the top of the canopy, resulting in an increased normalized velocity gradient near the ground and a decreased normalized velocity gradient at the top of the canopy (Fig. 4). The increased wind velocity within and below the canopy and the changes in the canopy profile shape are consistent with previous observations and simulation results that have investigated the effect of reduced canopy drag in neutral or near neutral flow (Raupach et al., 1986; Gardiner, 1994; Finnigan, 2000; Dupont and Brunet, 2008). The differing canopy profile features observed as the bark beetle outbreak progressed eventually resulted in a shift in the canopy profile to one expected for a scenario with surface fuels present but no canopy. In general our findings suggest that regardless of the nature of the bark beetle attack, the loss of canopy biomass corresponds to increased wind velocity and a shift in the shape of the wind profile toward what is expected for a scenario with little to no canopy fuel present.

One significant difference between the evolution of the Slow/Patchy wind profile and the Rapid/Broad wind profile was the presence of a bulge in the velocity profile below 0.4H above the ground in the Slow/Patchy scenario (Fig. 4). This bulge was more pronounced in our Slow/Patchy mortality scenario because it is exacerbated by considerable aggregation of the remaining live trees with large gaps between the clumps of trees. The clumps of

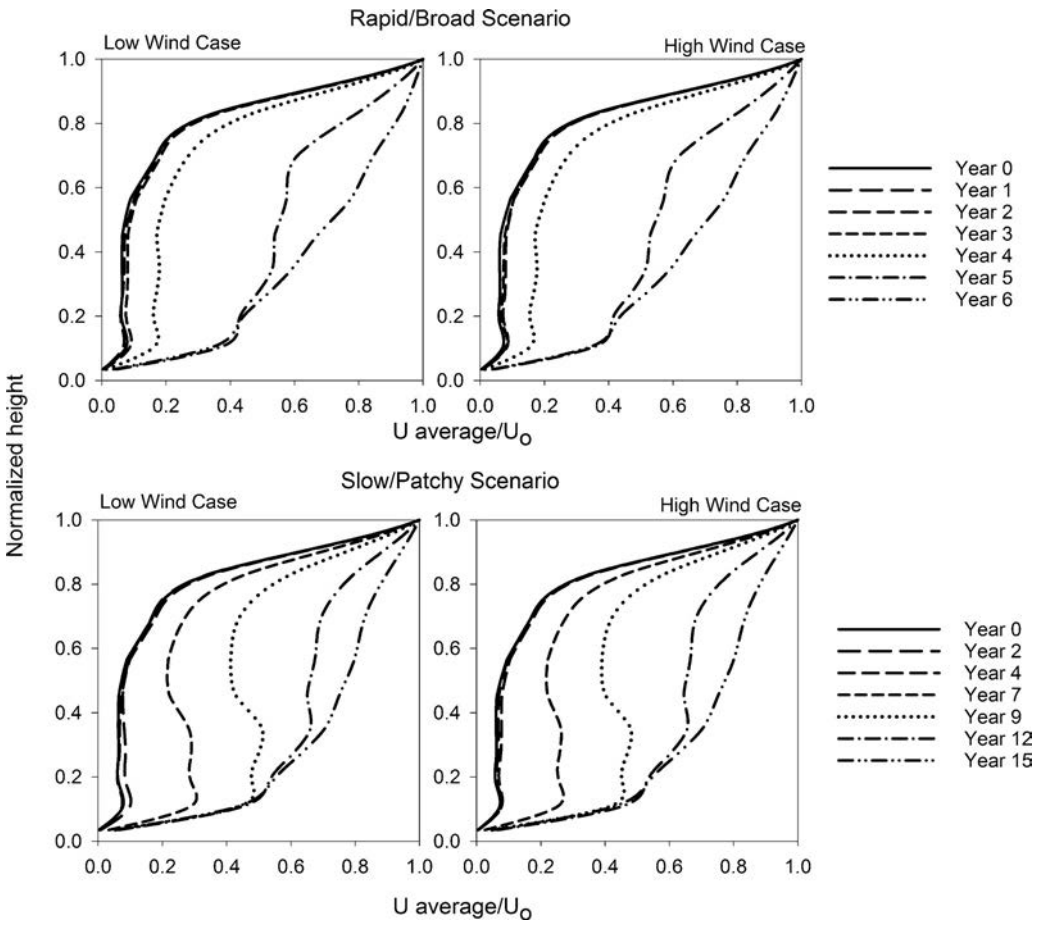

Fig. 4. Normalized vertical profiles of the streamwise wind velocity for the Rapid/Broad and Slow/Patchy scenarios for both the low and high wind speed cases.

Table 2
Mean streamwise wind velocities at the top of the canopy and mid-canopy height for the Rapid/Broad attack year 6 and the Slow/Patchy attack year 15 scenarios. The low wind speed and high wind speed cases had 12 and 24 m s^{-1} open wind speeds, respectively.

	Top of the canopy wind speed (m s^{-1})	Mid-canopy wind speed (m s^{-1})	Top of the canopy wind speed (m s^{-1})	Mid-canopy wind speed (m s^{-1})
	Low wind speed case		High wind speed case	
Rapid/Broad scenario year 6	6.1	4.4	11.8	8.3
Slow/Patchy scenario year 15	6.5	4.9	12.0	9.1

live trees acted as scoops, allowing sweeps of fast-moving air to swirl down into the gaps, intersect the clumps of live trees forcing the wind over, under, or through the next clump of trees. Some of this high-momentum air found its way through the trunk space where the bulk density asserting drag on the wind flow is much less than in the canopy resulting in the formation of the bulge in the velocity profile. This suggests that the pattern of mortality and the resulting forest structure are important factors controlling the within-canopy wind flow.

To evaluate the potential differences in mean wind velocity due to the spatial pattern of fuels created by the two mortality scenarios, we compared year 6 in the Rapid/Broad scenario to year 15 in the Slow/Patchy scenario. These two scenarios had similar canopy and surface fuel loadings but different horizontal and vertical spatial arrangements of canopy fuels, and thus, allowed us to investigate the potential impact of fuel heterogeneity on wind flow. More specifically the Slow/Patchy scenario resulted in a matrix of large canopy gaps whereas in the Rapid/Broad scenarios there were more remaining live trees and they were more evenly spaced. The Slow/Patchy scenario had greater wind velocities at both the top of the canopy and at the mid-canopy height compared to the Rapid/Broad scenario (Table 2). Given that the mean canopy and surface fuel loadings are the same in these two scenarios we attributed the differences in wind speed to the clumpy nature of fuels in the Slow/Patchy scenario which allowed for greater channeling of the wind within the canopy. This feature is less apparent in the low wind case because the entrainment of high momentum air into gaps and the subsequent redirection by the clump of trees is reduced. These findings are similar to the findings of Pimont et al. (2011) for more and less aggregated canopy densities. Based on these findings we hypothesize that for a given level of mortality, a bark beetle outbreak that results in a higher degree of aggregation of canopy fuels will result in greater within-canopy wind velocities, particularly under high wind velocity cases. However, future experimental studies are needed to confirm this hypothesis.

In addition to changes in the mean streamwise wind velocities there were also significant changes in the fluctuations in the U, V, and W velocities. Fig. 5 illustrates that in all of the mortality scenarios the ratio of streamwise-velocity correlation (twice the streamwise turbulent kinetic energy ($\overline{U'U'}$)) to the mean

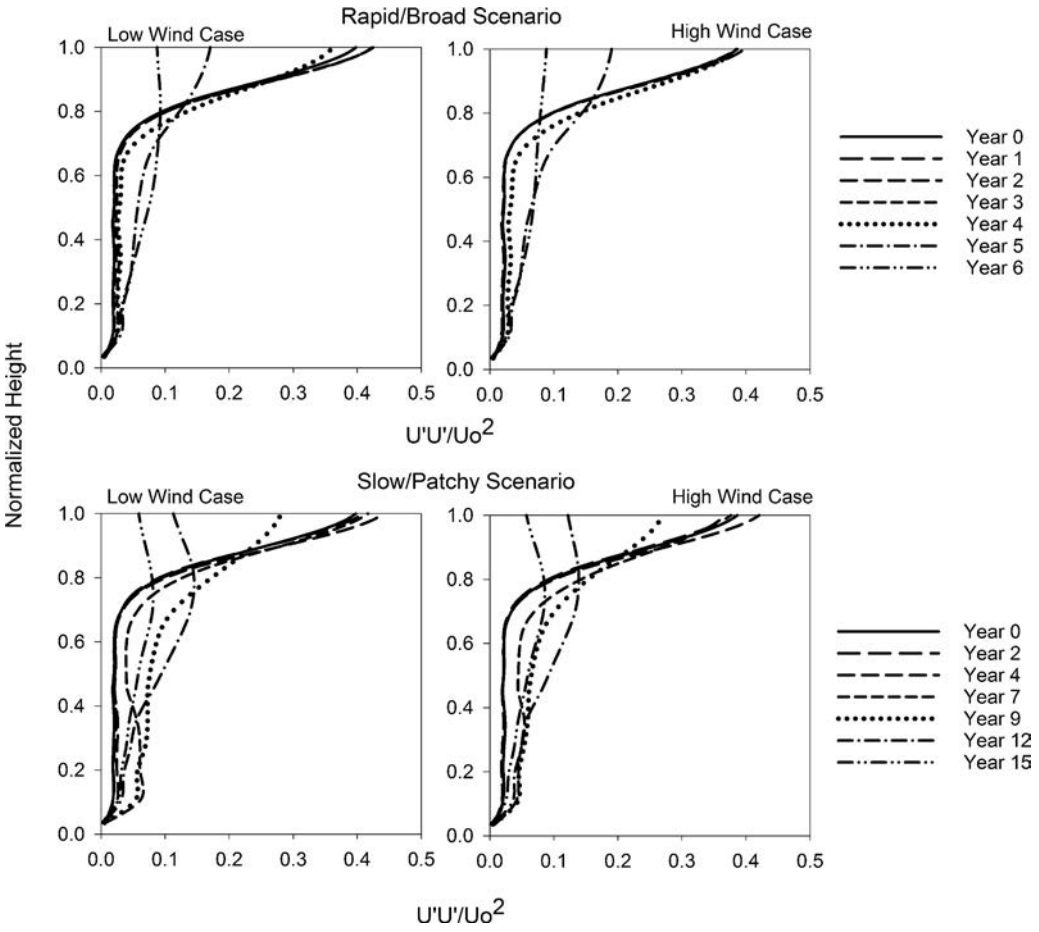

Fig. 5. Normalized vertical profile of the streamwise velocity correlation for the Rapid/Broad and Slow/Patchy scenarios for both the low and high wind speed cases.

kinetic energy at the top of the canopy was greatest initially at the top of the canopy where there was a strong mean shear. As mortality progressed and the canopy fuel loading decreased (after year 3), there was a corresponding decrease in the shear effect and the mean velocity and mean kinetic energy increased in the upper part of the canopy. This resulted in a reduction of the $U'\bar{U}'/U_0^2$ near the top of the canopy as the forest structure evolved. In the middle portion of the canopy this ratio increased after years 3 and 7 in the Rapid/Broad and Slow/Patchy scenarios, respectively, as winds started to intermittently penetrate the canopy and then intersect canopy fuels. In the Slow/Patchy scenario, the increased streamwise turbulence in the canopy relative to the mean kinetic energy at the top of the canopy was related to the growth of substantial gaps in the canopy where high velocity winds enter the canopy and are then diverted or redirected by the presence of tree clumps. As the tree clumps disappear near year 15 the normalized streamwise turbulence decreased in the mid canopy. In the Rapid/Broad scenario there was no formation of gaps and therefore the mid canopy maximum streamwise turbulence was much less pronounced in the slow wind case and nonexistent in the high wind case. The lack of the formation of gaps and clumps of trees combined with the reduction in canopy fuels resulted in the normalized streamwise turbulence growing monotonically to a maximum level in year 6 in the Rapid/Broad scenario. The Slow/Patchy scenario developed a bulge around $z = 0.2$ H related to the mean streamwise velocity bulge that occurred due to flow through the trunk space when there were well defined gaps in the canopy. This bulge is again not present in the Rapid/Broad scenarios.

The ratio of the cross-stream velocity correlation to the mean velocity at the top of the canopy, or normalized cross-stream turbulence ($V'\bar{V}'/U_0^2$), also generally decreased at the top of the canopy over time for both wind speed cases simulated (Fig. 6) for reasons similar to those described above for the normalized streamwise turbulence. At mid-canopy heights the normalized cross-stream velocity started to noticeably increase around years 4 and 7 for the Rapid/Broad and Slow/Patchy scenarios, respectively, and then decreased as the outbreak progressed and there was less fuel in the canopy. The peak normalized mid-canopy cross-stream velocity occurred due to the increased mean velocity shear associated with the loss of canopy biomass in successfully attacked trees and a scattering of living trees intersecting the flow. However, as additional mortality occurred, such as in the Slow/Patchy scenario, the normalized cross-stream turbulence at the mid canopy decreased ultimately approaching the pre-outbreak level in year 15. Difference in the normalized cross-stream turbulence between the two mortality scenarios is thought to be an effect of differences between aggregated trees forming clumps that cause minimal abrupt cross stream redirection of the flow in the Slow/Patchy scenario verses evenly dispersed individual trees in the Rapid/Broad scenario that cause more local disruption in the flow. Once again, the biggest difference in the normalized cross stream velocity of the two mortality scenarios was the pronounced bulge below 0.4 H in the profiles of the Slow/Patchy scenarios (especially the slow wind speed case) related to the formation of tree clumps separated by large gaps in the canopy.

The normalized vertical/streamwise cross correlation, also referred to as normalized vertical momentum flux ($U'W'/U_0^2$), showed similar trends to the normalized streamwise and cross-stream correlations in the later years of the Slow/Patchy scenarios and throughout the progression of the Rapid/Broad scenario (Fig. 7).

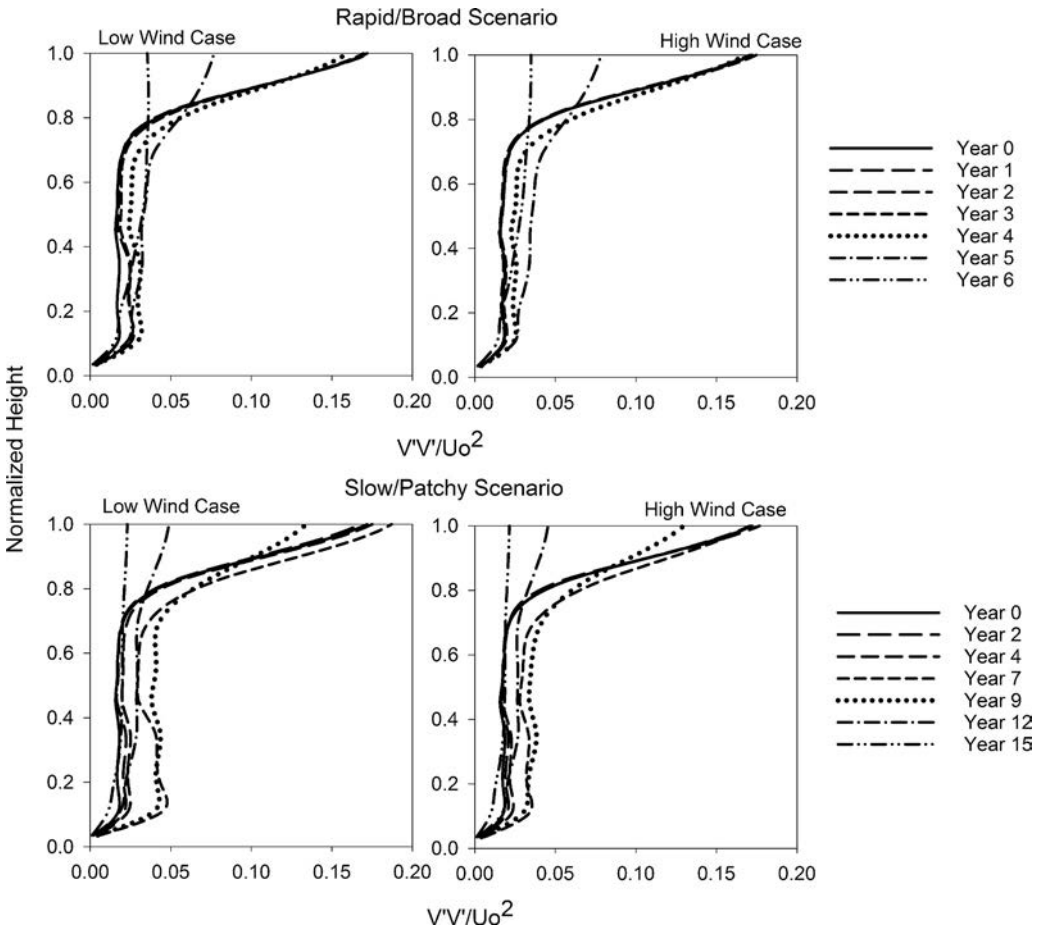

Fig. 6. Vertical normalized cross-stream correlation profile for the Rapid/Broad and Slow/Patchy scenarios for both the low and high wind speed cases.

For both bark beetle mortality scenarios, the normalized vertical momentum flux at the top of the canopy decreased throughout the progression of the outbreak compared to pre-outbreak. This decrease occurred due to both the reduced magnitude of the shear at the top of the canopy and an increase in the mean momentum within the canopy due to less drag present to dissipate the momentum, resulting in a reduction in the net flux of horizontal momentum down into the canopy to maintain the steady-state balance. One significant difference between this turbulence correlation and the streamwise or cross-stream correlations discussed above is in the Slow/Patchy scenario in year 7 where there was an overall increase in normalized magnitude of the vertical momentum flux compared to year 0, even near the top of the canopy. This is due to the opportunity for momentum to be entrained down into the canopy from the free stream above the canopy because of the presence of large canopy gaps, and the dissipation of momentum due to clumps of trees that limit free flow through the canopy.

Our results show that both the magnitude and pattern of bark beetle mortality influenced within canopy wind flow by reducing canopy density, and thus, the amount of vegetation imposing drag on the mean flow and by creating a mosaic of patches of vegetation and canopy gaps which resulted in localized wind channeling. To highlight the differences in the magnitude and timing of alterations to the within canopy wind flow between our two bark beetle mortality scenarios the mean and turbulent $z = 0.5\,H$ parameters are summarized through time in Fig. 8. Some of the key aspects of these differences include: (1) increased normalized turbulence levels from the initiation of the outbreak through years 9 and 6 during the Slow/Patchy and Rapid/Broad mortality scenarios, respectively, due to the loss of canopy biomass, and increased velocities within the canopy, and (2) reduced normalized turbulence following years 9 and 5 under the low wind speed cases during the Slow/Patchy and Rapid/Broad scenarios due to the persistence of the scattered living trees. This reduction was not present in the high wind speed case of Rapid/Broad scenarios where the winds had less time to react in the spaces between the trees. These findings highlight the potential implications that different levels of bark beetle mortality, rates of mortality, and the spatial patterns of mortality can have on the within canopy wind flow. Additional research that further explores the relationship between changes in the canopy biomass and spatial patterns with respect to changes in within canopy wind flow, as well as other biophysical processes are needed to fully understand the potential implications of disturbances such as bark beetles.

3.3. Effect of beetle attack progressions on simulated changes in fire behavior

There was a wide range of variation in the fire rate-of-spread (ROS) through time for both the Rapid/Broad attack and the Slow/Patchy attack scenarios for both wind speeds in the simulations (Fig. 9). In general both the Rapid/Broad and Slow/Patchy scenarios showed a similar trend across the temporal space simulated. Both scenarios showed an initial increase in the ROS soon after the initiation of the outbreak and a period of time where the ROS decreases compared to the initial stages of the outbreak. In some cases there was a subsequent increase in the ROS at the later stages of the outbreak (Fig. 9). The trends in ROS we found follow

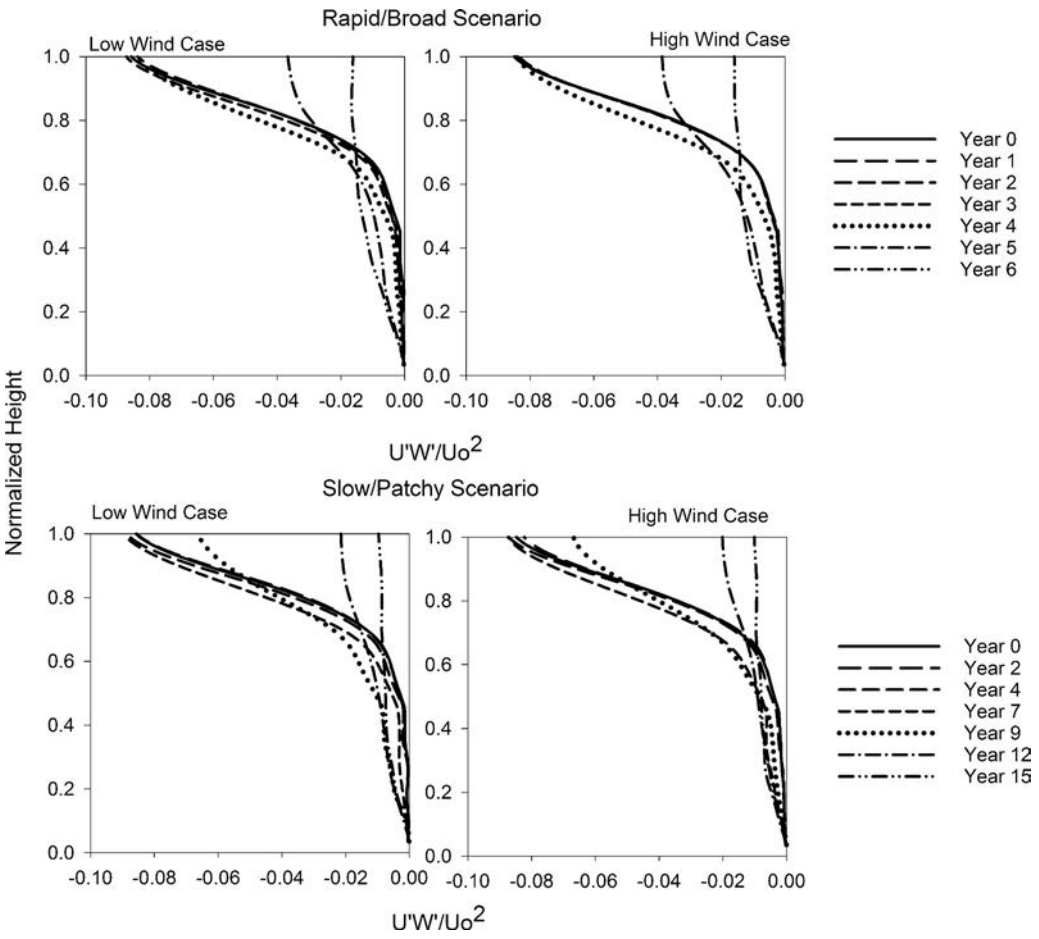

Fig. 7. Vertical profiles of the normalized vertical/streamwise cross correlation for the Rapid/Broad and Slow/Patchy scenarios for both the low and high wind speed cases.

hypothesized trends of crown fire potential through time for bark beetle affected forests (Jenkins et al., 2008; Hicke et al., 2012). However, our simulations suggest that there are differences in both the timing of peak ROS and the magnitude of those peaks across both the different bark beetle mortality scenarios and wind speed cases.

During the initial stages of the bark beetle outbreak (years 1–4), ROS depended on both the rate of mortality and the wind speed. In years 1 and 2, before there has been any change in canopy bulk density, and thus, no changes in canopy wind fields, the ROS decreased in the Slow/Patchy outbreak scenario but changed little in the Rapid/Broad scenario as compared to the pre-outbreak level. The decreased ROS for the Slow/Patchy scenario was in part caused by a reduction in foliar moisture content in widely dispersed locations, leading to the occasional torching of trees in both space and time. The torching of widely spaced dead trees along the fireline produced an increase in buoyancy-induced indrafts that altered heat transfer mechanisms, preventing the ignition of non-infested trees downwind, especially in the low wind cases, resulting in a reduction in the ROS. However, in the high wind speed case, the wind speed was sufficient to overcome the buoyancy-induced indraft created by the torching of isolated bark beetle infected trees and the ROS increased due to decreased canopy foliar moisture contents. In the Rapid/Broad scenario, ROS increased in year 3 under both wind speeds due to increasing level of mortality. The Rapid/Broad scenario also had a greater ROS compared to the Slow/Patchy scenario because of reduced mean canopy foliar moisture contents that resulted from the greater levels of mortality. The peak in ROS in year 3 for the Rapid/Broad scenario was due to continuity of dry fuels, and corresponded to a 1.8–2.7 fold increase in ROS compared to the pre-outbreak simulation for the low and high wind cases, respectively. In contrast to the Rapid/Broad scenario, the peak ROS for the Slow/Patchy scenario occurred in year 4 and was 1.2 and 2.0 times greater than the pre-outbreak level for the low and high wind cases. During these initial stages of the outbreak, the major difference between the two bark beetle mortality scenarios was a reduced mean foliar moisture content and greater connectivity between dead trees in the Rapid/Broad scenario. These findings suggest that the ROS is positively related to the level and continuity of bark beetle mortality and are consistent with results from Hoffman et al. (2012a). In addition, our findings suggest that models which use a spatially averaged value to broadly represent all the individual trees which make up the canopy fuels complex will produce different fire dynamics as compared to models that explicitly account for variations in the forest canopy. Future research efforts are needed to further understand the implications of these differences.

After year 3, the trends in ROS for the Rapid/Broad scenario diverged from the Slow/Patchy scenario due to the different evolutions of the canopy bulk density and canopy foliar moisture contents. For years 4 and 5, the amount and continuity of canopy fuels decreased considerably in the Rapid/Broad scenario resulting in a decreased ROS compared to the pre-outbreak level, despite increased wind penetration into the canopy. A decrease in ROS following the loss of canopy fuels associated with an increasing proportion of the trees being in the gray phase has been suggested by several past research studies (Jenkins et al., 2008; Hicke et al., 2012; Simard et al., 2011). Following the peak ROS in year 4, the ROS in the Slow/Patchy scenario also decreased as a result of lower canopy continuity associated with the loss of canopy biomass. Although the

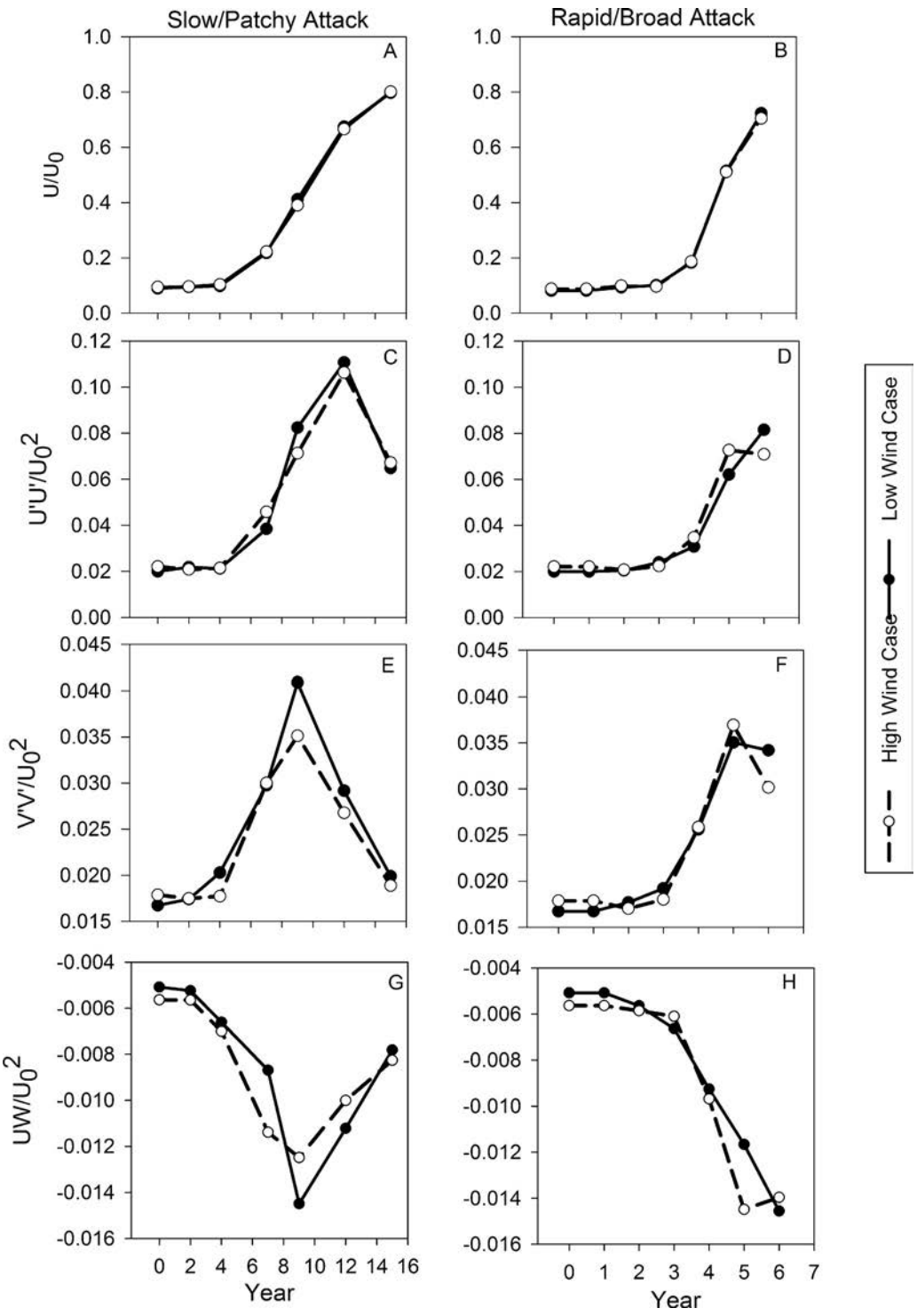

Fig. 8. Temporal trends of the: normalized streamwise wind speed at 0.5 H for the Slow/Patchy (A) and Rapid/Broad (B) outbreak scenarios, normalized streamwise velocity correlation at 0.5 H for the Slow/Patchy (C) and Rapid/Broad (D) outbreak scenarios, normalized cross stream velocity correlation at 0.5 H for the Slow/Patchy (E) and Rapid/Broad (F) outbreak scenarios and the normalized vertical/streamwise cross correlation at 0.5 H for the Slow/Patchy (G) and Rapid/Broad (H) outbreak scenarios under low and high winds.

peak increase in ROS for the Slow/Patchy scenario occurred one year after the peak ROS for the Rapid/Broad scenario, both arose before a significant loss of canopy fuel occurred in the stand, and both declined with loss of canopy continuity.

Following additional loss of canopy biomass in year 6 for the Rapid/Broad scenario for the high wind speed case, the fire ROS increased by 5% compared to the pre-outbreak scenario (Fig. 9). However, in the low wind speed scenario the fire rate of spread was 60% lower than the pre-outbreak scenario. The additional loss of canopy biomass in years 7–12 for the Slow/Patchy scenario resulted in similar patterns of ROS as the Rapid/Broad scenario. For the low wind speed case the ROS decreased between 21 and 44% during this time compared to the pre-outbreak scenario. While

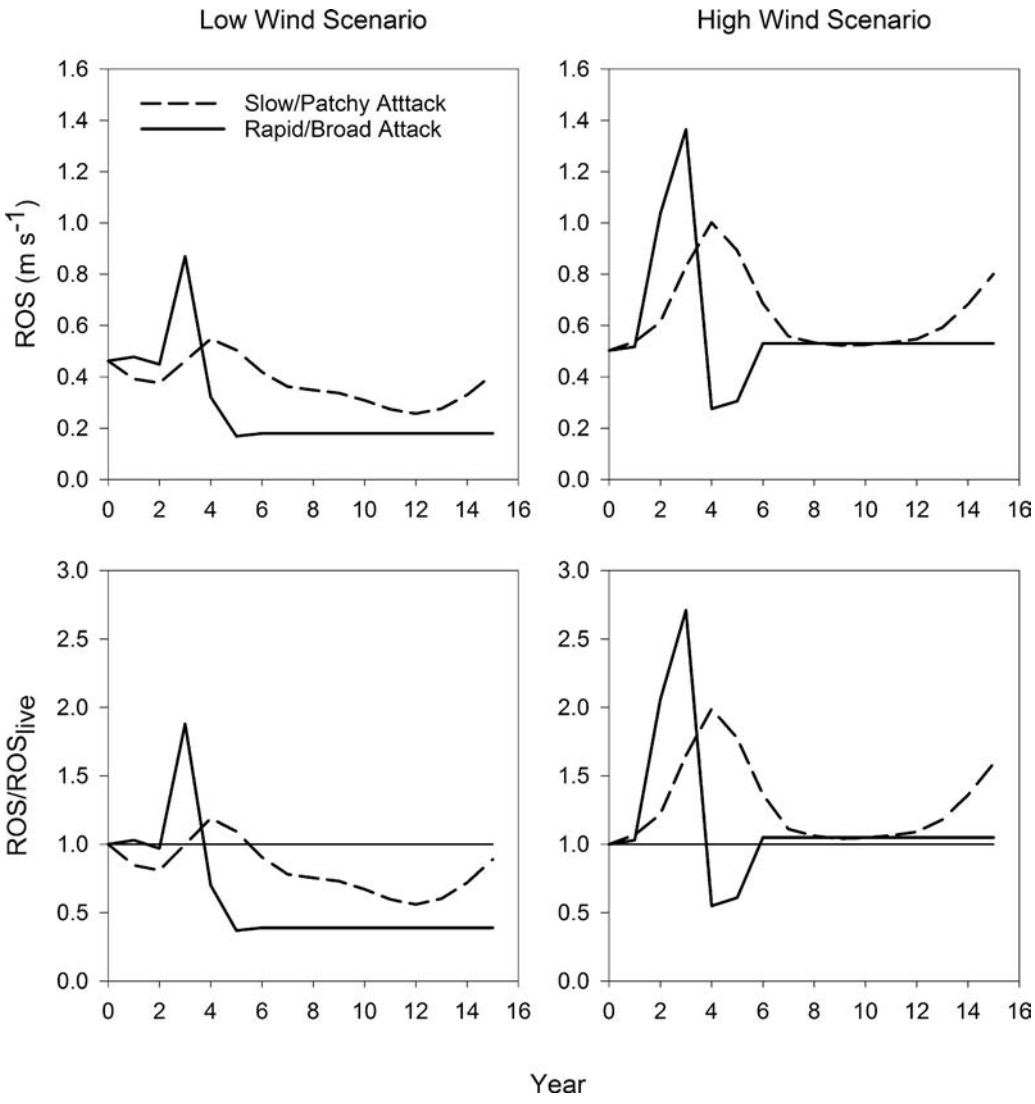

Fig. 9. Simulated rates of fire spread and normalized rates of fire spread through time following a bark beetle outbreak for the Rapid/Broad and Slow/Patchy scenarios for low and high wind speed cases. The curves for the Rapid/Broad attack were extended beyond year 6 for illustrative purposes.

for the high wind speed scenario the ROS was between 3 and 10% greater than the pre-outbreak scenario. These findings highlight the potential impact of wind velocity on the effect bark beetle mortality has on ROS.

Following year 12, both the low and high wind speed cases showed an increase in the ROS as compared to years 7-12. In the high wind speed case, this resulted in a 60% increase of ROS compared to the pre-outbreak level, whereas the low wind speed case had a ROS that was 11% lower compared to the pre-outbreak level. The recovery in ROS for the Slow/Patchy scenarios is likely occurring due to increased penetration of winds into the canopy and greater near surface wind velocities. This is similar to the increased ROS in year 6 for the Rapid/Broad scenario. However, the increase in year 12 of the Slow/Patchy scenario was much greater than that of year 6 for the Rapid/Broad scenario due to the stronger winds near the surface and the aggregated canopy fuels. However, increased ROS during the later years of these simulations for the Slow/Patchy scenario may not be realistic since we did not consider the degradation of surface fuels or the response of vegetation through time. Additional research that investigates the sensitivity of temporal trends in fire behavior following bark beetle outbreaks is needed to better understand the variability in fuels complex responses and the associated impacts on fire behavior.

Our data suggest that the maximum ROS occurs when there is high canopy bulk density and low mean canopy foliar moisture content (Fig. 10). This combination of parameters is most likely to occur during the initial stages of an outbreak (years 1–3) that closely resembles the Rapid/Broad scenario or in years 1–5 for a situation that resembles the Slow/Patchy scenario. In addition, our simulations as well as other research (Hoffman et al., 2012a) suggest that fire behavior during the early phases of an outbreak is positively related to the level of mortality. As an outbreak progresses, the canopy bulk density decreases, the canopy foliar moisture content increases due to a loss of dead fuels, and there is increased wind penetration into the canopy. These changes resulted in higher near-surface wind velocities as well as increases in the energy requirements for crown ignition and spread leading to reduced ROS as compared to the initial phases of the outbreak. This pattern is in agreement with several past studies that have investigated the temporal trends in crown fire potential following bark beetle outbreaks (Jenkins et al., 2008; Hicke et al., 2012). However, in spite of a decrease in ROS during the later portion of the outbreak compared to the initial phases, our simulations suggested that the ROS

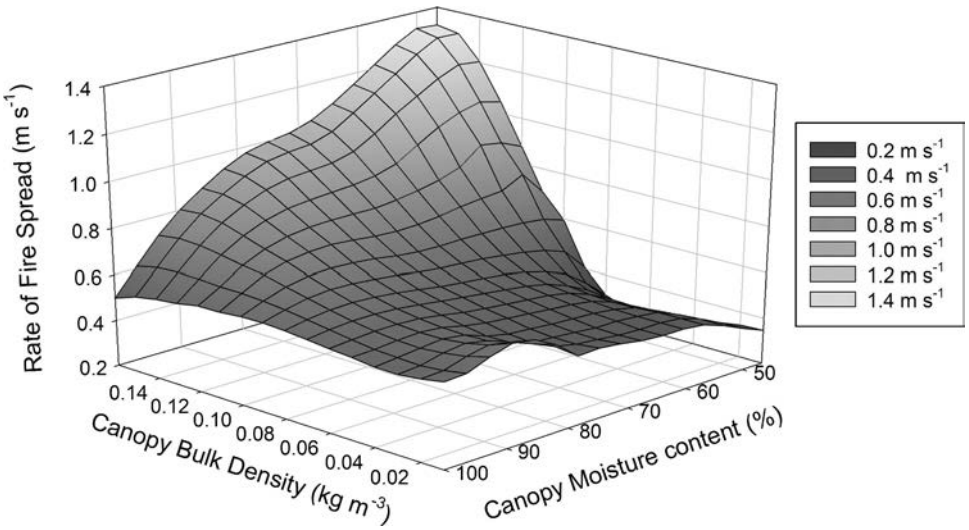

Fig. 10. Rate of fire spread as a function of canopy bulk density and mean canopy fuel moisture, based on all 28 scenarios at low and high wind speeds.

can remain above the pre-outbreak level, particularly under high wind velocities. The potential for increased fire behavior potential during the latter stages of an outbreak, when most trees are in the gray phase, has been suggested by Jenkins et al. (2012) and Linn et al. (2013).

Despite an increasing amount of research into the effects of bark beetle outbreaks on fuels and fire behavior over the last decade, there remains a lack of experimental field data that can be used to assess predictions and hypotheses derived from various modeling approaches. Recently Perrakis et al. (2014) published data on 14 crown fires that occurred in lodgepole pine-dominated forests during the initial phases of an outbreak (between 1 and 5 years following mortality). Although the particulars of the mortality progression, wind profiles, and fuels complex are not well documented or potentially even known for these experiments, these data provide much needed real world measurements in bark beetle infested areas (Hicke et al., 2012; Hoffman et al., 2012a, 2013; Page et al., 2014) and provide a starting point for at least qualitatively assessing if model predictions are at least realistic. The observed mean rate of spread from the 14 experiments from Perrakis et al. (2014) was 0.41 m s^{-1} with a standard deviation of 0.24, with wind velocities ranging from 1 to 7 m s^{-1} at 10 m above the ground in clearings. In addition, Perrakis et al. (2014) compared their experimental data to the expected fire behavior for pre-outbreak lodgepole pine forests and determined that during this period there would be an approximate 2.6 fold increase in the ROS as compared to pre-outbreak conditions. For the same time period in our simulations, our mean predicted rates of spread were 0.45, 0.66 for the Rapid/Broad and 0.46 and 0.71 m s^{-1} for the Slow/Patchy low and high wind speed cases, respectively (Fig. 11), with wind speeds ranging from 3 to 4 m s^{-1} for the low wind speed cases and 7–9 m s^{-1} in the high wind cases at heights 10 m above the canopy. The standard deviations of our simulations were 0.23, 0.44, for the Rapid/Broad and 0.10 and 0.26 for the Slow/Patchy low and high wind speed cases, respectively (Fig. 11). Given that our high wind speed cases had greater wind velocities than those reported for the experiments

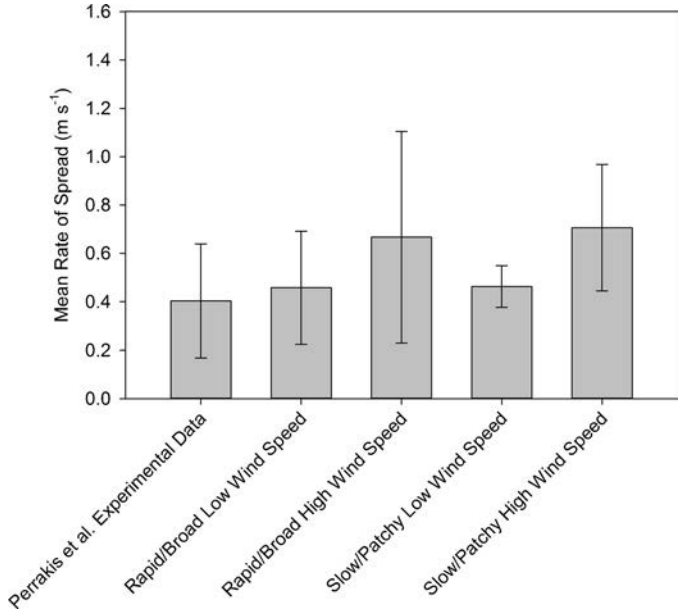

Fig. 11. Comparison of mean rate-of-spread predictions (±1 standard deviation) for our Rapid/Broad and Slow/Patchy low and high wind speed scenarios from FIRETEC to experimental data from 14 fires in mountain pine beetle-infested forests (Perrakis et al., 2014).

it is rational that the simulated rates of spread for our high wind speed scenarios would be greater than those reported by Perrakis et al. (2014). In addition our simulations show an increase in rate of spread of between 1.2 and 2.7 compared to the pre-outbreak simulations depending upon the bark beetle mortality scenario and the wind speed. Despite the relatively small sample size of the wildfire observations available ($n = 14$) and the lack of details regarding many important variables thought to influence fire behavior, this comparison provides a qualitative check that our simulations, are at least reasonably consistent (i.e., within a similar order of magnitude) with our expectations of the real world system. It is important to acknowledge, however, that although comparisons such as the ones made above are useful for general insight, they do not constitute a validation of the model, primarily because the details associated with the experimental data place limits on model testability. The level of fidelity of the validation of any fire model will depend upon the fidelity of the characterization of the dynamic and heterogeneous environment that controls the fire. Future experiments that provide more detailed information regarding the fuels complex, wind fields and fire behavior in bark beetle affected stands are needed for model evaluation in both early and latter periods of time following an outbreak. It is our hope that the results of this investigation will inspire, prompt, and guide future observations that would be focused on discerning the realities of the interactions between wind and fire in these evolving heterogeneous mortality events.

4. Conclusions

A total of 28 simulations were conducted using FIRETEC, a coupled fire/atmosphere model, in order to explore the ways in which a bark beetle outbreak may influence the within-canopy winds and the rate of fire spread in lodgepole pine-dominated forests. These simulations represented two broad evolutions of a bark beetle outbreak that resulted in different spatio-temporal fuels complexes consisting of various mixtures of yellow, red, brown, gray and green trees. To quantify the effect of these fuel complexes on fire behavior we used two different ambient wind speeds. In addition we provided a qualitative comparison of our simulated ROS with recent experiments conducted during the initial time phases following an outbreak.

The simulated changes in canopy structure through time resulted in alterations to the average wind profile as well as the wind fluctuations within the canopy. In general, wind speeds were lower in the initial phases of an outbreak before significant canopy biomass was removed. As the beetle outbreak progressed there was an increasing loss of biomass in the canopy imposing drag on the wind flow which lead to increased mid-canopy and near-surface wind velocities in both bark beetle outbreak scenarios. However, for a given amount of canopy biomass, we found that outbreaks that resulted in a patchy or aggregated distribution of living and dead trees had greater near-surface wind velocities than more evenly spaced patterns of fuels due to differences in wind entrainment and channeling. Scenarios where large gaps in the canopy were separated by groups of trees resulted in increases in the wind speed fluctuations and increased stem-space velocities compared to more evenly-distributed but similar fuel loads. These findings highlight two potential mechanisms by which bark beetle mortality can influence within canopy wind flow: first by reducing the amount of vegetation present in the canopy that acts as a source of wind drag, and second by altering spatial patterns of vegetation in a manner that leads to wind channeling, which also additionally affects the overall wind drag. This suggests that a function computing in-canopy wind velocities based simply on the amount of biomass present, but no spatial distribution information, may not account for differences in near-surface wind flow associated with various mortality patterns. This could lead to an under prediction bias of fire rates of spread, particularly in fuels that are characterized as aggregated.

Both the rate of bark beetle mortality and the ambient wind speed played a significant role in determining the ROS following the initiation of a bark beetle outbreak by altering the heat requirements for ignition and convective heat transfer processes. The initial phases following an outbreak consist of minimal reductions in canopy biomass and a general decrease in the heat requirements for crown ignition which resulted in increased rates of spread during this period of time, with the greatest increases occurring for the Rapid/Broad scenario. Interestingly, in both scenarios the peak rate of spread occurred before significant canopy biomass loss. As additional canopy biomass was removed, there were changes in the convective heating of unburned vegetation and the fire rate-of-spread decreased from the peak ROS which occurred in the initial phases of the outbreak. However, under high wind speeds, this reduction resulted in elevated spread rates as compared to pre-outbreak levels. These findings suggest that the changes in canopy bulk density and mean canopy foliar moisture content associated with various rates of mortality, along with the ambient wind velocity, exert considerable influence on the relative change in ROS through time. Given the potential variation in wind flow and predicted rate of fire spread due to changes in the severity and timing of mortality, we suggest that future studies investigating the impact of bark beetle mortality should report the severity or amount of mortality along with the rate of mortality through time (Wulder et al., 2009). In the absence of such data a more thorough description of the mixture of individual tree phases within the study area could also be useful. The inclusion of this data into future studies could help clarify existing knowledge gaps related to the effect of bark beetle outbreaks and explain potential differences in the reported effects of bark beetle outbreaks on fire behavior through time (Hicke et al., 2012).

Acknowledgments

This research was funded by the USDA Forest Service Research (both Rocky Mountain Research Station and Washington office), National Fire Plan Dollars through Research Joint Venture Agreement 11-JV-11221633-207 with Colorado State University, and Interagency Agreements09-IA-11221633-215 and 13-IA-11221633-103 with Los Alamos National Laboratory. Los Alamos National Laboratory's Institutional Computing Program provided computational resources to complete this project.

References

Bone, C., White, J.C., Wulder, M.A., Robertson, C., Nelson, T.A., 2013. Impact of forest fragmentation on patterns of mountain pine beetle-caused tree mortality. Forests 4, 279–295.

Brown, J.K., 1970. Ratios of surface area to volume for common fine fuels. For. Sci. 16 (1), 101–105.

Brown, J., 1975. Fire cycles and community dynamics in lodgepole pine forests. In: Baumgartner, D. (Ed.), Management of Lodgepole Pine Ecosystems: Symposium Proceedings. Washington State Cooperative Extension Service, pp. 429–456.

Cassagne, N., Pimont, F., Dupuy, J.L., Linn, R.R., Mårell, A., Oliveri, C., Rigolot, E., 2011. Using a fire propagation model to assess the efficiency of prescribed burning in reducing the fire hazard. Ecol. Modell. 222 (8), 1502–1514.

Cole, W.E., Amman, G.D., 1980. Mount Ain Pine Beetle Dynamics in Lodgepole Pine Forests. General Technical Report INT-GTR-89. USDA Forest Service Intermountain Forest and Range Experiment Station, Ogden, UT.

DeRose, R.J., Long, J.N., 2009. Wildfire and spruce beetle outbreak: simulation of interacting disturbances in the central Rocky Mountains. Ecoscience 16 (1), 28–38.

Donato, D.C., Harvey, B.J., Romme, W.H., Simard, M., Turner, M.G., 2013. Bark beetle effects on fuel profiles across a range of stand structures in Douglas-fir forests of Greater Yellowstone. Ecol. Appl. 23 (1), 3–20.

Dupont, S., Brunet, Y., 2008. Edge flow and canopy structure: a large-eddy simulation study. Boundary-Layer Meteorol. 126 (1), 51–71.

Finnigan, J., 2000. Turbulence in plant canopies. Annu. Rev. Fluid Mech. 32, 519–571.
Gardiner, B.A., 1994. Wind and wind forces in a plantation spruce forest. Boundary-Layer Meteorol. 67 (1–2), 161–186.
Geiszler, D.R., Gara, R.I., 1978. Mountain pine beetle attack dynamics in lodgepole pine. In: Berryman, A.A., Amman, G.D., Stark, R.W. (Eds.), The Ory and Practice of Mountain Pine Beetle Management in Lodgepole Pine forests. University of Idaho, Moscow, Idaho, pp. 182–187.
Geiszler, D.R., Gallucci, V.F., Gara, R.I., 1980. Modeling the dynamics of mountain pine beetle aggregation in a lodgepole pine stand. Oecologia 46, 244–253.
Graf, M., Reid, M.L., Aukema, B.H., Lindgren, B.S., 2012. Association of tree diameter with body size and lipid content of mountain pine beetles. Can. Entomol. 144 (3), 467–477.
Hicke, J.A., Johnson, M.C., Hayes, J.L., Preisler, H.K., 2012. Effects of bark beetle-caused tree mortality on wildfire. For. Ecol. Manage. 271, 81–90.
Hoffman, C., Morgan, P., Mell, W., Parsons, R., Strand, E.K., Cook, S., 2012a. Numerical simulation of crown fire hazard immediately after bark beetle-caused mortality in lodgepole pine forests. For. Sci. 58 (2), 178–188.
Hoffman, C.M., Sieg, C.H., McMillin, J.D., Fulé, P.Z., 2012b. Fuel loadings 5 years after a bark beetle outbreak in south-western USA ponderosa pine forests. Int. J. Wildland Fire 21 (3), 306–312.
Hoffman, C.M., Morgan, P., Mell, W., Parsons, R., Strand, E., Cook, S., 2013. Surface fire intensity influences simulated crown fire behavior in lodgepole pine forests with recent mountain pine beetle-caused tree mortality. For. Sci. 59 (4), 390–399.
Jenkins, M.J., Hebertson, E., Page, W., Jorgensen, C.A., 2008. Bark beetles, fuels, fires and implications for forest management in the Intermountain West. For. Ecol. Manage. 254 (1), 16–34.
Jenkins, M.J., Page, W.G., Hebertson, E.G., Alexander, M.E., 2012. Fuels and fire behavior dynamics in bark beetle-attacked forests in Western North America and implications for fire management. For. Ecol. Manage. 275, 12.
Johnson, P.C., Coster, J.E., 1978. Probability of attack by southern pine beetle in relation to distance from an attractive host tree. For. Sci. 24 (4), 574–580.
Jolly, W.M., Parsons, R.A., Hadlow, A.M., Cohn, G.M., McAllister, S.S., Popp, J.B., Hubbard, R.M., Negron, J.F., 2012. Relationships between moisture chemistry, and ignition of *Pinus contorta* needles during the early stages of mountain pine beetle attack. For. Ecol. Manage. 269, 52–59.
Keane, R.E., Reinhardt, E.D., Scott, J., Gray, K., Reardon, J., 2005. Estimating forest canopy bulk density using six indirect methods. Can. J. For. Res. 35 (3), 724–739.
Klutsch, J.G., Battaglia, M.A., West, D.R., Costello, S.L., Negrón, J.F., 2011. Evaluating potential fire behavior in lodgepole pine-dominated forests after a mountain pine beetle epidemic in north-central Colorado. W. J. Appl. For. 26 (3), 101–109.
Linn, R.R., 1997. A Transport Model for Prediction of Wildfire Behavior. LA-13334-T. Los Alamos National Laboratory, Los Alamos, NM.
Linn, R.R., Cunningham, P., 2005. Numerical simulations of grass fires using a coupled atmosphere–fire model: basic fire behavior and dependence on wind speed. J. Geophys. Res. D: Atmos. (1984–2012) D13, 110.
Linn, R.R., Winterkamp, J., Colman, J., Edminster, C., 2005. Modeling interactions between fire and atmosphere in discrete element fuel beds. Int. J. Wildland Fire 14 (1), 37–48.
Linn, R.R., Sieg, C.H., Hoffman, C.M., Winterkamp, J.L., McMillin, J.D., 2013. Modeling wind fields and fire propagation following bark beetle outbreaks in spatially-heterogeneous pinyon–juniper woodland fuel complexes. Agric. For. Meteorol. 173, 139–153.
Logan, J.A., Bentz, B.J., Powell, J.A., 1998. Model analysis of spatial patterns in mountain pine beetle outbreaks. Theor. Pop. Bio. 53, 236–255.
Mell, W., Jenkins, M.A., Gould, J., Cheney, P., 2007. A physics-based approach to modelling grassland fires. Int. J. Wildland Fire 16 (1), 1–22.
Mell, W., Maranghides, A., McDermott, R., Manzello, S.L., 2009. Numerical simulation and experiments of burning Douglas fir trees. Combust. Flame 156 (10), 2023–2041.
Mitchell, R.G., Preisler, H.K., 1991. Analysis of spatial patterns of lodgepole pine attacked by outbreak populations of the mountain pine beetle. For. Sci. 37 (5), 1390–1408.
Negrón, J.F., Popp, J.B., 2004. Probability of ponderosa pine infestation by mountain pine beetle in the Colorado Front Range. For. Ecol. Manage. 191 (1), 17–27.
Page, W., Jenkins, M.J., 2007. Predicted fire behavior in selected mountain pine beetle-infested lodgepole pine. For. Sci. 53 (6), 662–674.
Page, W.G., Jenkins, M.J., Alexander, M.E., 2014. Crown fire potential in lodgepole pine forests during the red stage of mountain pine beetle attack. Forestry 87 (3), 347–361.
Perrakis, D.D.B., Lanoville, R.A., Taylor, S.W., Hicks, D., 2014. Modeling wildfire spread in mountain pine beetle-affected forest stands, British Columbia, Canada. Fire Ecol. 10 (2), 1–26.
Pimont, F., Dupuy, J.L., Linn, R.R., Dupont, S., 2009. Validation of FIRETEC wind-flows over a canopy and a fuel-break. Int. J. Wildland Fire 18 (7), 775–790.
Pimont, F., Dupuy, J.L., Linn, R.R., 2011. Impacts of fuel-break structure on wind-flows and fire propagation simulated with FIRETEC. Ann. For. Sci. 68 (3), 523–530.
Raffa, K.F., Aukema, B.H., Bentz, B.J., Carroll, A.L., Hicke, J.A., Turner, M.G., Romme, W.H., 2008. Cross-scale drivers of natural disturbances prone to anthropogenic amplification: the dynamics of bark beetle eruptions. Bioscience 58 (6), 501–517.
Raupach, M.R., Coppin, P.A., Legg, B.J., 1986. Experiments on scalar dispersion within a model-plant canopy. 1. The turbulence structure. Boundary-Layer Meteorol. 35 (1–2), 21–52.
Reinhardt, E., Scott, J., Gray, K., Keane, R., 2006. Estimating canopy fuel characteristics in five conifer stands in the western United States using tree and stand measurements. Can. J. For. Res. 36 (11), 2803–2814.
Rothermel, R.C., 1972. A Mathematical Model for Predicting Fire Spread in Wildland Fuels., Research Paper INT-115. USDA, Forest Service Intermountain Forest and Range Experiment Station, Ogden, UT.
Rothermel, R.C., 1983. How to Predict the Spread and Intensity of Forest and Range Fires, GTR-INT-143. USDA, Forest Service Intermountain Forest and Range Experiment Station, Ogden, UT.
Rothermel, R.C., 1991. Predicting behavior and size of crown fires in the Northern Rocky Mountains, Research Paper INT-438. USDA, Forest Service Intermountain Forest and Range Experiment Station, Ogden, UT.
Safranyik, L., Silversides, R., McMullen, L.H., Linton, D.A., 1989. An empirical approach to modeling the local dispersal of the mountain pine beetle (*Dendroctonus ponderosae* Hopk.) (Col. Scolytidae) in relation to sources of attraction, wind direction and speed. J. Appl. Entomol. 108 (1–5), 498–511.
Schoennagel, T., Veblen, T.T., Negron, J.F., Smith, J.M., 2012. Effects of mountain pine beetle on fuels and expected fire behavior in lodgepole pine forests, Colorado, USA. PLoS One 7 (1), e30002.
Scott, J.H., Reinhardt, E.D., 2001. Assessing Crown Fire Potential by Linking Models of Surface and Crown Fire Behavior, Research Paper RMRS-RP-29. USDA Forest Service Rocky Mountain Research Station, Fort Collins, CO.
Simard, M., Romme, W.H., Griffin, J.M., Turner, M.G., 2011. Do mountain pine beetle outbreaks change the probability of active crown fire in lodgepole pine forests? Ecol. Monogr. 81 (1), 3–24.
Van Wagner, C.E., 1977. Conditions for the start and spread of crown fire. Can. J. For. Res. 7 (1), 23–34.
Wulder, M.A., White, J.C., Grills, D., Nelson, T., Coops, N.C., Ebata, T., 2009. Aerial overview survey of the mountain pine beetle epidemic in British Columbia: communication of impacts. BC J. Ecosyst. Manage. 10 (1), 45–58.